Ultra fast laser machined hydrophobic stainless steel surface for drag reduction in laminar flows

R.Jagdheesh[1*],B.Pathiraj[1] ,A.G.Marin[2], D. Arnaldo del Cerro[1], R.G.H.Lammertink[3], D. Lohse[2]

A.J. Huis in 't Veld[1], G.R.B.E Römer[1]

[1]*University of Twente, Faculty of Engineering Technology, Chair of Applied Laser Technology, P.O. Box 217, 7500 AE, Enschede, The Netherlands*

***Email** : J.Radhakrishnan@ctw.utwente.nl

[2] *Department of applied Physics,University of Twente, Physics of Fluids Group, Enschede, P.O. Box 217, 7500 AE, Enschede, The Netherlands*

[3] *Department of Chemical Engineering, University of Twente, Membrane science and Technology Group, P.O. Box 217, 7500 AE, Enschede, The Netherlands*

Kew words: laser patterning, contact angle, drag reduction, Hydrophobic, Microstructure

Abstract

Hydrophobic surfaces have attracted much attention due to their potential in microfluidics, lab on chip devices and as functional surfaces for the automotive and aerospace industry. The combination of a dual scale roughness with an inherent low-surface-energy coating material is the pre-requisite factor for the development of an artificial superhydrophobic surfaces. Ultra short pulse laser (USPL) machining/structuring is a promising technique to obtain the dual scale roughness. Moreover, ultra short laser pulses allow machining without or with limited thermal effects. Flat stainless steel (AISI 304L) were laser machined with ultraviolet laser pulses of 6.7ps, at different laser processing parameters. Next, the samples were coated with a monolayer of perfluorinated octyltrichlorosilane (FOTS) to get a superhydrophobic surface. The degree of hydrophobicity was accessed by static contact angle measurement. Laser patterned surface has longitudinal micro channels. Drag reduction in liquid flow can be obtained due to the shear free boundary condition at air-liquid menisci. The geometry of the patterns was analyzed with optical and scanning electron microscopy. Micro-Particle Image Velocimetry (μPIV) has been employed to measure and visualize the flow over such patterns

1.Introduction

Surface morphology is a key factor determining the wettability of a solid surface. The wettability of a solid surface is usually addressed by measuring the static contact angle measured between the water droplet and the solid surface. In general, a hydrophilic surface has contact angle less than 90° and a hydrophobic surface more than 90°. Superhydrophobic surfaces have more than 150° contact angle [1]. The Wettability of the solid surface mainly depends on two factors: surface topology and chemistry [2,3]. Hydrophobic surfaces have attracted much attention due to their potential in microfluidics, lab on chip devices and as functional surfaces for the automotive and aerospace industry. Patterning is the one of the effective ways to change the topography and improve the hydrophobicity of the metal surface.

In recent years, inspired by the topography of the lotus leaf, numerous methods like plasma surface modification, radiation grafting, various coatings methods, electrochemical deposition, electroless replacement deposition, Lithographically patterned substrates, vertically aligned carbon nanotubes, nanocasting and extruding of polymers, natural oxidation and laser patterning have been adopted for development of hydrophobic surfaces [4-22]. Among these surface modification techniques, laser patterning is a unique technique which can modify the topology with very minimum distortion to the bulk material. Moreover, it is a non contact, very precise and complex patterns can be structured on the surface. The nano scale ripples found on the laser patterned surface are comely known as laser induced periodic surface structure (LIPSS), which can be observed near the ablation threshold. In most cases the orientation of the regular ripples are found to be perpendicular to the polarization direction of incident laser beam [23].

Successful attempts were made by Baldacchini et al. in converting a hydrophilic silicon surface to hydrophobic by applying a fluorosilane coating on laser textured surface [24]. The conversion of hydrophilic to hydrophobic surface was also achieved without additional coating on the surface after laser treatment [25]**.** Wettability from hydrophilic to hydrophobic was also obtained by Bhattacharya et al. on hydrophobic clustered-copper nanowires without using a hydrophobic coating. The transition was purely a geometrical phenomenon related to the nature of clustering[26]. Kietzig et al.

studied time dependency of hydrophobicity on structure created by femtosecond laser machining on different metals and alloys. They observed that, the laser induced dual scale roughness structures plays a significant role in the wetting properties of the metal surfaces [27]. Wu and Zhou showed that surfaces with double scale structure showed higher apparent contact angle [28].

Hydrophobicity of solid surfaces follow either the Cassie-Baxter model [29] or the Wensel model [30]. According to Wensel model, the liquid is in contact with the whole surface and hydrophobicity of a solid surface is improved by an increase in solid/liquid interfacial area due to the surface roughness. For the Cassie-Baxter model, the surface has voids in which air trapped, where the liquid cannot penetrate. In this case, instead of solid/liquid interface, it has solid/liquid and liquid/vapor interface. Therefore, if the surface roughness has regular patterns of square or conical protrusions (pillars), air can be trapped inside the valleys and it follows the Cassie-Baxter model.

2. Laser machining

Ultra short pulse laser (USPL) machining/structuring is a promising technique to obtain micro-pattern on a metal surface. In this paper, we investigate the development of hydrophobic surface on flat stainless steel plates for drag reduction in laminar flow. Micro-particle Image Velocimetry (µPIV) was employed to measure the effective slip lengths achieved on such patterns.

3. Experiment

Flat stainless steel (AISI 304L) plates were laser machined by ultraviolet laser pulses of 6.7ps, with different laser processing parameters. The samples were coated with perfluorinated octyltrichlorosilane (FOTS) to get a hydrophobic surface. The geometry of the patterns was analyzed with optical and scanning electron microscopy. The samples where in the size of 60mm × 20mm × 1mm were used for the laser patterning experiments. Before the laser irradiation, samples were mechanically polished with SiC grinding paper (starting from 600-1200 grit) and finally by colloidal silica particles resulting in surface roughness of R_a = 80nm. The samples were cleaned with acetone prior to laser machining.

A frequency-tripled (wavelength: 343nm) Trumpf TruMicro Nd:YAG laser with an average power of 15W was used for this experiment. Machining in ultraviolet range reduces the localized heating and melting. Moreover, shorter wavelength allows smaller diffraction-limited spot sizes and therefore fine features in the surface. The experiments were performed at fixed pulse duration of 6.7ps. The linearly polarized laser beam was guided over the samples by a two mirror galvo scanner system (Fig.1) and the angle of incidence was 90°.

The laser beam has Gaussian power density profile. Microchannels were fabricated with a effective spot size of 18µm. Laser machining was performed in a clean room at atmospheric conditions. The laser processing parameters were optimized by experimenting with different laser power and scan speeds. The laser processing conditions are shown in Table.1.

Table I. Laser processing parameters.

Sample name	Power (mW)	Fluence J/cm^2	SS m/s	RR (kHz)	No. OS
PIV03	150	0.2	300	200	50
PIV04	150	0.2	300	200	100

SS : Scan speed, RR: pulse repetition rate, OS: Over scan

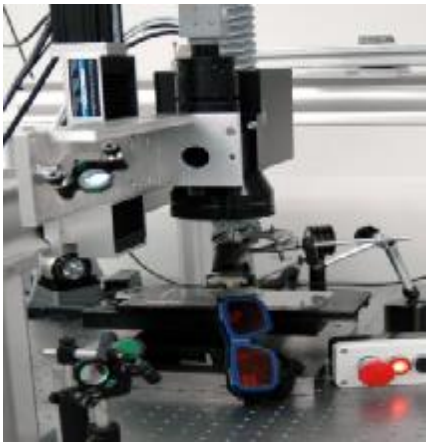

Fig.1. Galvo scanner setup for laser Micromachining experiments.

The laser machined samples were analyzed with scanning electron microscope (SEM), Optical microscope and confocal microscopy to evaluate the microstructure and the geometry of the microchannels.

Before measuring the static contact angle (CA), the samples (PIV03 and 04) were silanized in a oven using silane reagent (Trichloro (1H, 1H, 2H, 2H-perfluoroocty) to reduce the surface energy. The hydrophobicity of the solid surface was evaluated by a video based optical contact angle measuring device, (the OCA 15 plus of Data Physics Instruments) with distilled water droplets of 10µl each.

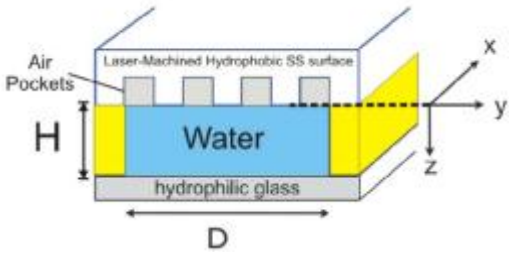

Fig. 2. Laminar flow over Laser-Machined SS structure.

The experimental set to assess the drag reduction is sketched in Fig. 2 and 3. A laminar flow of thickness H is created between the micromachined hydrophobic structure and a thin glass which will permit visualization. The liquid consists of degassed milli-Q water seeded with 300 nm diameter fluorescent polystyrene particles (R300, Thermo), with a peak excitation wavelength of 542 nm (green) and a peak emission wavelength 612 nm (red). The particles are designed with a mass density of 1.05 g/cm^3, which makes them practically neutrally buoyant tracers allowing follow the flow field. To generate a steady laminar flow, a water flow rate of 1 µL/min (PHD 2000 Infusion syringe pump, Harvard Apparatus) is injected between the micromachined structure and the glass wall.

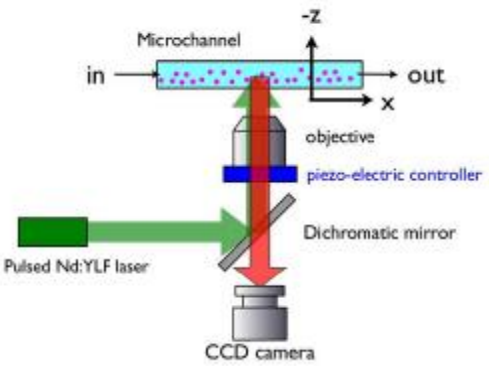

Fig. 3. Optical set up for µPIV measurements and visualization.

The measuring system is depicted in fig.3. image pairs of the seeding particles are observed with properly delated double-pulsed laser illumination via an objective and recorded by a CCD camera. The scanning plane of the laser illumination is controlled by a piezo-electric controller to investigate the particle motions in the x−y plane at the different channel heights z. The cross-correlation of these captured image pairs allows us to quantification of the flow field. The channel illumination is produced by a dual cavity diode-pumped Nd:YLF laser at 527nm (Pegasus-PIV, New Wave Re-search Co) via an oil immersion Plan-Apochromat 100×objective with numerical aperture NA = 1.4 (Carl Zeiss), mounted in an inverted microscope (Carl Zeiss, Axiovert 40 CFL). The particles absorb green laser light and emit in the red spectrum, which passes through a dichromatic mirror into the CCD camera. With a proper delay time Δt between two exposures, image pairs were recorded by a cooled sensitive double shutter CCD camera with the resolution 1376 × 1040 pixels × 12 bit (Sensicam PCO Imaging). Typical Δt in the experiments ranged from 1 ms to 25 ms depending on the distance from the walls. The precise focusing in the desired plane over the microchannel was controlled by an accurate piezoelectric objective-lens positioning system (MIPOS 500, Piezosystem Jena GmbH) with the resolution of 100 nm. The field of view of µ-PIV images was about 120 µm × 127µm. When processing data, small windows of the typical size of 64 × 16 pixels (~ 8 × 2 µm) were used to achieve high spatial resolution for resolving detailed velocity fields. Interrogation windows were overlapped by 50% to satisfy the Nyquiest sampling criterion [28]. Each velocity field in 4 a plane at the different channel height z was processed from 150 − 200 image pairs so as to reduce the random vectors due to Brownian thermal motion.

4 Results and Discussion

4.1. Optimization of Laser Parameters (Power, scan speed and no. over scans)

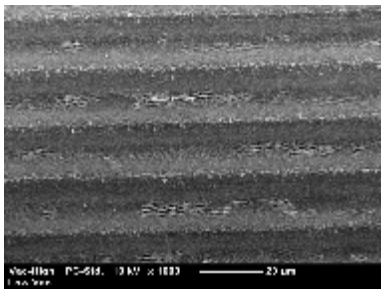

Fig. 4. SEM micrograph of sample treated at 50mW power with a scan speed of 200mm/s (Energy/pulse: 0.25 µJ, No. of OS:40)

Figure 4 shows the SEM micrograph one of the sample. In order to avoid debris and the redeposited metal vapour, laser machining was performed with relatively low power and relatively high scan rate. Figure 4 shows the SEM picture for the sample machined at low power and relatively high scan rate (50mW power with a scan speed of 200mm/s) and it is free from debris redeposited metal vapour. Nevertheless, the top of the microchannels were wide open and the water droplet can easily penetrate into the channel and flush out the air in the pockets trapped in the microchannels. Therefore, a relatively high power and high scan rate is required for micromachining experiments. The sample produced with the power of 150mW at 300 mm/s scan rate

found to show a good surface morphology with dual scale features on the surface (Fig.7).

4.2. Optimization of the geometry of the pattern with respect to CA measurement.

Influence of Varying hatch distance

As a first step to produce a superhydrophobic surface, it is essential to optimize the geometry of the pattern in terms of contact angle of the laser machined surface. Different samples were prepared with varying hatch distance ranging from 20 to100 µm by keeping all the other parameters constant as listed in Table I. Since, the fresh laser machined surface exhibited hydrophilic behavior [26] the contact angle measurement was performed after 10 days from the time of sample preparation. Figure 5 represents the CA as a function of hatch distance.

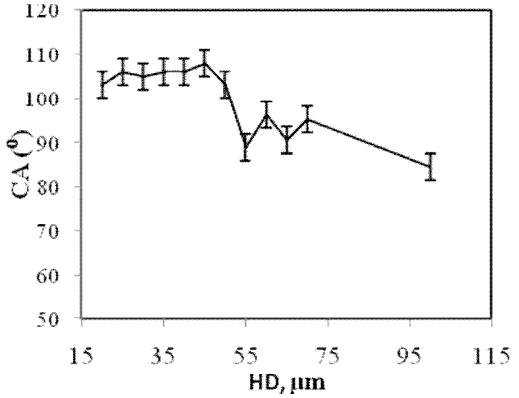

Fig 5. Contact angle as function of hatch distance.

The samples show a consistent hydrophobic behavior until the a hatch distance of 50 µm and it tend to decrease above that value. This experiment gives the range of hatch distance which yield hydrophobic surfaces. For microfluidic applications, it is essential to have the microchannels with minimum width and maximum depth as possible in order to trap air inside the microchannels which lead to the composite interface between liquid, solid and air. Therefore, it is required to find out the maximum depth of the channel in terms of CA measurement.

Influence of Varying laser Over scans (OS)

The depth of the microchannels can be improved/increased by increasing the number of over scans. To evaluate the depth of the microchannels in terms of CA measurement a range of samples have been produced with increasing the number of over scan ranging from 20-100. Figure 6 shows the contact angle as function of number of over scans. Laser micromachining was performed at different OS by keeping all the other laser parameters constant. The contact angle recorded for the sample prepared with OS of 40, 50 and 60 are well pronounced.

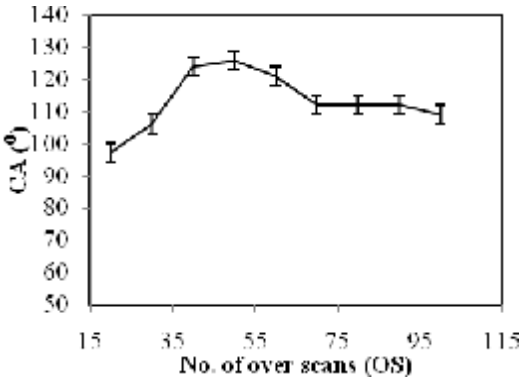

Fig. 6. Contact angle as function of OS.

As the no. of OS increases beyond 60 times, the CA tends to decrease. This may be caused by the redeposited materials on the surface as well as inner part of the channels and the top of the channel was wide open leading to easy penetration of water into the channel. As the number of OS is increased, the depth of the cannel would increase and the material ablated from the bottom of the channel would be trapped inside the channel. This would result in random roughness, which may tend to decrease the hydrophobicity of laser machined surface. Analyzing the samples prepared at different hatch distances and different scan speed in terms of CA, the samples produced at smaller hatch distance with 50 over scans shows appreciable improvement in hydrophobicity. Since the drag reduction experiments demand for the microchannels with minimum width and maximum depth, it was decided to fabricate the microchannels with 18µm width (minimum diameter of the laser spot with the available optics at the µ-lab) and 50 OS.

4.3. Fabrication of microchannels with optimized laser parameters.

Two samples (PIV03 and 04) were prepared for the µ-Particle Image Velocimetry (µ PIV) measurement with different aspect ratios. The variation in the aspect ratio is achieved through increasing the depth of channel by increasing the number of over scans.

Figure 7 shows the SEM image of microchannels fabricated. The depth and width of the channels are in micrometer range. Nano scale ripples are observed at the top and the bottom of the microchannels. Moreover, on the top of the micro channels, redeposited metal can be observed. The microchannels are is tapered. This is caused by the Gaussian energy density distribution of the focused beam. This is the prime reason for the tapered edge of the microchannles. Debris and the redeposited material is observed on the top of the microchannels, which is unwanted. The density of the loosely bound particles on the surface is reduced by adopting single step "cleaning" with the same laser parameters used

for micromaching. Figure 8 shows a SEM image of the sample with reduced redeposited material on the top of the microchannels. The remaining particles on the top surface can be cleaned by increasing the number of over scans, but, the material removal from the top of the microchannels may have adverse impact on the geometry of the microchannels.

Cross sectional examinations were performed to analyze the depth and the width of the channels. Figure 9 shows the optical micrograph of the cross section of sample PIV03. The measured width is about 20µm and depth is about 14µm in average. The cross sectional examination also reveals no sign of redeposited material on the top of the channels. A confocal image of the microchannels is shown in figure 10. The nanoscale ripples can be seen on the bottom of the microchannel. The depth information obtained from the confocal image is in good agreement with the cross sectional examination of the microchannels.

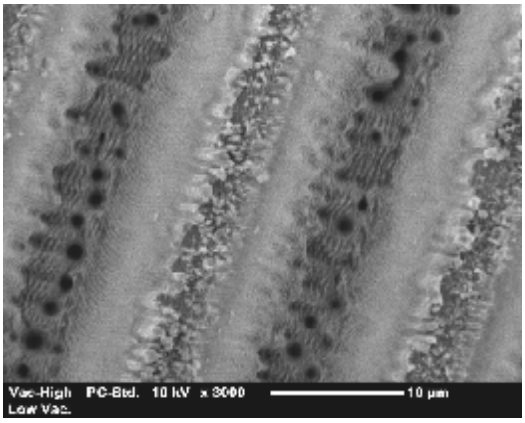

Fig.7. SEM Picture of sample PIV03, after laser machining, before cleaning.

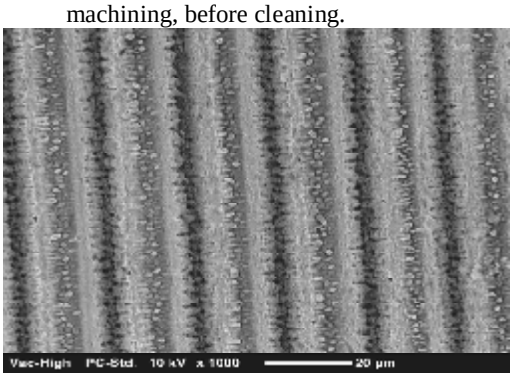

Fig. 8. SEM image of sample PIV03, after single step cleaning.

Contact angle measurements were performed on the surface of silanized laser textured and non textured FOTS coated samples. The volume of the water droplet was 10µl. The plain (untextured) stainless steel exhibited a contact angle of 116° (fig.11A) and the textured sample showed a contact angle of 130° (fig.11B) on average.

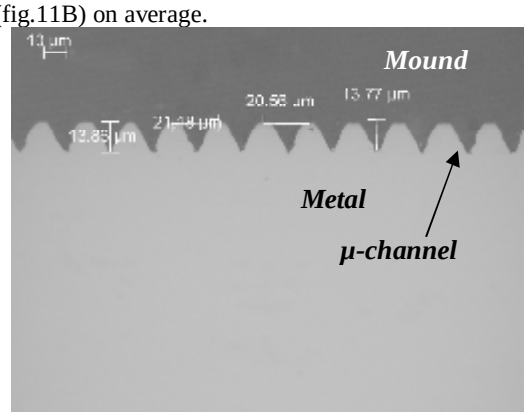

Fig 9. Cross sectional optical micrograph of sample PIV03

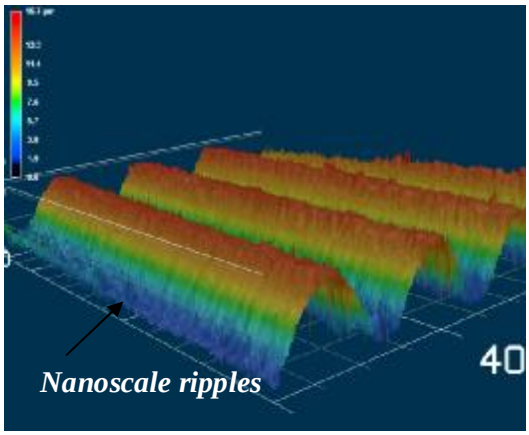

Fig. 10 . Confocal 3D image of microchannels, sample PIV03.

3.3.4.CA measurement

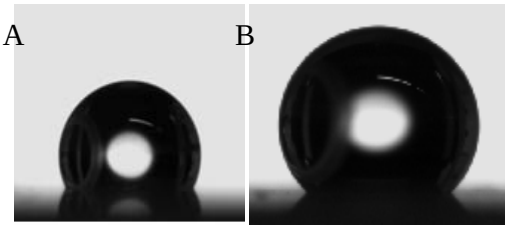

Fig. 11. Photographs of water droplet on FOTS coated plain SS(A) plate and laser machined microchannels (B).

The improvement in the textured samples is due to the composite interface between air, solid and water. From the cross sectional analysis, it is understood that there are microchannels of depth of about 13 µm and the water droplet would suspend on the projections with the air pockets trapped inside the microchannels.

Micro-Particle Image Velocimetry (µPIV) is often used to measure the effective violation of the non-slip condition over solid surfaces. In this case, the liquid is expected to flow without invading the air

pockets, maintaining the minimum contact with the solid walls. This is however not always achieved in experimental conditions despite the high static contact angles found. Although the microchannel configuration was tested in the μPIV system, better stability was found with an structure consisting of uncommunicated microholes of diameters of approximately 12 microns and center-to-center distance of around 15 microns. The results to be shown will demonstrate that the surface is able to hold such a non-wetting state during long times, which will eventually give rise to an effective drag reduction. Measurements of slip-length are currently being done using the micro-PIV system to quantify the effect.

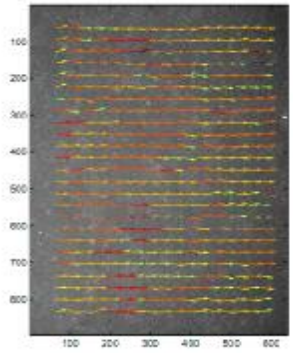

Fig 12. Raw data from μPIV measurement.

In fig. 12, a typical μPIV measurement image (100 μm x 78 μm) is shown, at a distance of 10 μm from the hydrophobic structure. The oscillating values of the velocity along the horizontal manifests the alternation of solid areas with free surface areas, with periodicity coinciding with the air pockets' size. Additionally it has been checked that the air pockets remain intact over of several hours. Slip-length measurements are currently being done to quantify the drag reduction effect over these substrates.

4. Conclusion

The laser machined microchannels found to have nano-scale ripples on the bottom and side walls of the channels and it is free from micro-cracks. The FOTS coated laser patterned micro channels exhibited a static contact angle about 130°. The μPIV visualization and measurements reveal a flow with great stability and potentiality as a substrate with reduced friction. This observation is expected to be confirmed by the slip-length measurements.

Acknowledgement

This work was carried out as a "Strategic Impact Project (SIP)" of the Institute of Mechanics, Process and Control Twente (IMPACT) of the university of Twente , Netherlands.

References

[1] M. Miwa, A. Nakajima, A. Fujishima, K. Hashimoto, T. Watanabe, Langmuir, 16,(2000) 5754.
[2] Y. Thmos, Philos. Trans. R. Soc. London, 95, (1805) 65.
[3] R.N. Wenzel, Ind. Eng. Chem., 28, (1936) 988.
[4] Benson RS, Nucl. Instrum. Methods Phys. Res Sect. B, 191,(2002)752.
[5] F.Arefi-Khonsari,M.Tatouliana,F.Bretagnol, O.Bouloussa,F.Ronadlez Surf.Coat.Technol.,200, (2005)14.
[6] D.Pappas,A.Bujanda JD.Demaree,JK.Hirvonen W.Kosik, R.Jensen, S.McKnight, Surf Coat.Technol.,201,(2006)4384.
[7] N G. Semaltianos,W. Perrie,P. French, M.Sharp,G.Dearden,K.G.Watkins, Appl. Surf. Sci., 255,(2008) 2796.
[8] C.H. Wang, Y.Y. Song, J.W. Zhao, X.H. Xia, Surf. Sci. 600,(2006) 38.
[9] L. Wang, S.J. Guo, X.G. Hu, S.J. Dong, Electrochem. Commun.10,(2008) 95.
[10] N. Zhao, F. Shi, Z.Q. Wang, X. Zhang, Langmuir, 21,(2005)4713.
[11] Q.M. Pan, Y.X. Cheng, Appl. Surf. Sci., 255 (2009) 3904.
[12] W. Song, J.J. Zhang, Y.F. Xie, Q. Cong, B. Zhao, J. Colloid Interface Sci., 329,(2009) 208–211.
[13] Q.M. Pan, M. Wang, H.B. Wang, Appl. Surf. Sci. 254, (2008)6002.
[14] W.C. Wu, M. Chen, S. Liang, X.L. Wang, J.M. Chen, F. Zhou, J. Colloid Interface Sci.,326, (2008)478.
[15] Z.G. Guo, F. Zhou, J.C. Hao, W.M. Liu, J. Colloid Interface Sci. 303, (2006) 298.
[16] Q. Wang, B.W. Zhang, M.N. Qu, J.Y. Zhang, D.Y. He, Appl. Surf. Sci. 254 (2008)2009.
[17] D.K. Sarkar, M. Farzaneh, R.W. Paynter, Mater. Lett. 62,(2008)1226.
[18] G.X. Li, B. Wang, Y. Liu, T. Tan, X.M. Song, H. Yan, Appl. Surf. Sci.,255(2008)3112.
[19] D.Oner, T.McCarthy., J. Langmuir,16,(2000), 7777.
[20] R.Fu¨rstner,W.Barthlott,C. Neinhuius,P.Walzel, Langmuir, 21,(2005) 956.
[21] K.K.S.Lau,J. Bico,K.B.K.Teo, M.Chhwalla, G. Amaratunga, W.I.Milne,G.H. McKinley,K.K.Gleason, Nano Lett., 2003, *3*, 1701.
[22] H. Li,X.Wang, Y.Song,Y. Liu,Q.Li, L.Jiang, D.Zhu, Angew.Chem., Int. Ed. 40,(2001) 1743.
[23]Z.Guosheng,P.M.Fauchet,A.E.Siegman,phys.Rev.B (10)(1982)5366
[24] T.Baldacchini, J.E. Carey, M.Zhou, E.Mazur, Langmuir 2006, 22, 4917.
[25] V.Zorba, L.Persano, D.Pisignano, A.Athanassiou, E. Stratakis, R.Cingolani, P. Tzanetakis, C. Fotakis, Nanotechnology,17(2006)3234.
[26] P.Bhattacharya, S.Gohil, J.Mazher, S.Ghosh, P.Ayyub,.Nanotechnology, 19,(2008) 075709.
[27] A.M. Kietzig, S.G. Hatzikiriakos, Peter Englezos, Langmuir 25 (2009)4821.
[28] B.Wu, M. Zhou, J.Li ,X.Ye, G. Li, L.Cai, Appl. Surf. Sci 256 (2009) 61–66
[29] A.B.D. Cassie,S.Baxter,Trans. Faraday Soc. 40,(1944) 546.
[30] R.N.Wenzel, Ind. Eng. Chem., 28,(1936)988.